Chapter 31
Energy Dissipation of a System with Foam to Metal Interfaces

Laura D. Jacobs, Robert J. Kuether, and John H. Hofer

Abstract The physical mechanisms of energy dissipation in foam to metal interfaces must be understood in order to develop predictive models of systems with foam packaging common to many aerospace and aeronautical applications. Experimental data was obtained from hardware termed "Ministack", which has large, unbonded interfaces held under compressive preload. This setup has a solid aluminum mass placed into two foam cups which are then inserted into an aluminum can and fastened with a known preload. Ministack was tested on a shaker using upward sine sweep base acceleration excitations to estimate the linearized natural frequency and energy dissipation of the first axial mode. The experimental system was disassembled and reassembled before each series of tests in order to observe the effects of the assembly to assembly variability on the dynamics. There are some important findings in the measured data: there is significant assembly to assembly variability, the order in which the sine sweeps are performed influence the dynamic response, and the system exhibits nontrivial damping and stiffness nonlinearities that must be accounted for in modeling efforts. A Craig-Bampton model connected with a four-parameter Iwan element and piecewise linear springs is developed and calibrated using test data with the intention of capturing the nonlinear energy dissipation and loss of stiffness observed in experiment.

Keywords Energy dissipation • Harmonic loading • Contact friction • Craig-Bampton model • Model validation

31.1 Introduction

Electronic and electromechanical components are packaged in foam to prevent excessive vibration amplitudes during transportation and operation. Solid foams are used to package defense components per MIL-STD 2073 [1]. This packaging leads to foam/metal interfaces, which have long been recognized as significant contributors to energy dissipation. The mechanisms for energy dissipation in these systems include friction, impacts and the large material damping common in most foams. Standards, such as MIL-STD 810G [2], require qualification of military components under vibration environments in their packaging. To be able to model and understand how systems containing foam to metal interfaces will respond to various vibration environments, it is important to understand the energy dissipation mechanisms and their effect on the dynamics. Currently, modeling capabilities to capture the dissipative behavior of metal parts in foam are being developed. Physical experiments are crucial to validate models and gain an understanding of the physical phenomena required for modeling.

A simple system, called "Ministack", consisting of a solid aluminum mass placed in two foam cups that are then inserted into an aluminum can, is developed to represent a metal part packaged in foam. Ministack contains a small number of interfaces and is a relatively simple geometry to model. The simplicity of the design enables the study and explanation of the physics through experimentation and computational modeling. Details of Ministack are described in Sect. 31.2.

Experiments with Ministack, utilizing sinusoidal excitation to measure the energy loss per cycle in a manner similar to that reported by other investigators [3–12] are performed. The experiments performed on Ministack investigate the influence of several different parameters, including: amplitude of excitation, snugness of fit, load path, and sequence of testing. For each configuration, a series of upward sine sweep base accelerations at different amplitudes are performed, exciting the first axial mode of the system. Acceleration data is collected at the top of Ministack and analyzed to determine the natural frequency and energy dissipation of the system. Section 31.3 presents the resulting data from the experiments.

Sandia is a multiprogram laboratory operated by Sandia Corporation, a Lockheed Martin Company, for the United States Department of Energy under contract DE-AC04-94AL85000.

L.D. Jacobs (✉) • R.J. Kuether • J.H. Hofer
Sandia National Laboratories, P.O. Box 5800 MS 0557, Albuquerque, NM 87185, USA
e-mail: ldjacob@sandia.gov

M. Allen et al. (eds.), *Dynamics of Coupled Structures, Volume 4*, Conference Proceedings of the Society for Experimental Mechanics Series, DOI 10.1007/978-3-319-29763-7_31

A Craig-Bampton reduced order model [13] of Ministack is developed in Sect. 31.4 with the intention of capturing the loss of stiffness in the interface as well as the nonlinear energy dissipation as the amplitude of excitation increases. The interface between the solid mass and foam cups is modeled with two gap elements, otherwise known as piecewise linear springs, and a four-parameter Iwan element [14]. The parameters of these constitutive models are calibrated based on the measured transfer functions in order to see whether a simplified model can capture the salient nonlinear behavior.

31.2 Experimental Setup

To create a system with a dominant axial mode that exercises the large foam to metal interfaces, a solid aluminum mass is placed in foam cups and then inserted into an aluminum can, as illustrated in Fig. 31.1. A preload is then applied to the steel disk on the top of the foam cups using a press, and then a threaded steel ring is tightened to secure the preload. The aluminum can has an inner diameter of 10 cm, an outer diameter of 12.7 cm and a depth of 15.2 cm. The can is welded to a square plate that has nine bolt holes (Fig. 31.1) to allow the specimen to be attached to a shaker. The plate has a recess in the bottom of it (not shown) to accommodate a uniaxial accelerometer to control the input acceleration. A triaxial accelerometer is placed on top of the solid mass to measure the response of the system. The steel disk has a hole in the middle to allow for the accelerometer cable to exit the specimen.

31.2.1 Foam Specimen Details

The foam specimens are made from 320 kg/m^3 closed cell PMDI foam. The foam specimens are in two parts, a top half which has an access hole for attaching an accelerometer and a bottom half which has a solid bottom. The two halves are cup-like in nature with an outer diameter of 10 cm and an inner diameter of 7.62 cm. The bottoms and sides of the cups are 12.7 mm thick. The surface of the foam specimens is friable.

Two different depths of cups are used in the experiment. One set of foam specimens has an interior depth of 5 cm. Nominally, the solid mass would fit exactly in the specimens yielding parallel load paths of through the solid mass and through the foam. However, with machining tolerances, there are cases where the load path is either through the foam alone or through the mass alone in addition to the cases of parallel load paths. The second set of foam specimens were manufactured to have a smaller interior depth of 4.68 cm. Nominally, there would be a 6.35 mm gap between the two pieces of foam, thus ensuring a load path through the solid mass even with variations due to machining tolerances.

Fig. 31.1 Test specimen

31.2.2 Solid Mass Details

Three solid masses of different diameters are used in the experiments to determine the effects of snugness of fit on the frequency and energy dissipation characteristics of the system. The nominal, or no gap, specimen has a diameter of 7.62 cm, so that it fits snugly in the foam specimens. The 1.5875 mm gap specimen has a diameter of 7.46 cm so that there is a gap between the solid mass and the foam. The 3.175 mm gap specimen has a diameter of 7.30 cm. All three solid masses are 10 cm in length and are made from 6061-T6 Aluminum. They have a recessed area in the top that can accommodate a triaxial accelerometer.

31.2.3 Specimen Assembly

The solid mass is placed in both halves of the foam cups, with markings on the cups being lined up to help limit the variability in alignment from assembly to assembly. Then, the cups are placed in the can, with markings on the cups and the can being aligned to help with the repeatability of assembly. The steel plate is placed on top of the foam and solid mass assembly in the can, after which a load cell is placed on top of the assembly. A preload is applied using a press until the reading on the load cell is approximately the nominal preload. The retaining ring is tightened to maintain the preload, the press is released, and Ministack is ready for testing.

31.2.4 Test Specifications and Data Collection

During testing, Ministack is oriented so that the plate on the bottom is flat on the shaker. In this orientation the specimen is being excited in the direction of the load path. The energy dissipation comes from the foam rubbing against the metal interface as well as the interface between the two sets of foam for the cases when there is contact.

A constant acceleration sine sweep base excitation is run from 500 to 3000 Hz at a rate of 3 octaves per minute (an octave represents a doubling of frequency). The sweep rate allows for the test article to experience several cycles at each frequency, allowing for sufficient data at each frequency to estimate the natural frequency and energy dissipation. Four different amplitudes, 1 g, 2 g, 5 g and 10 g, are used to determine the effects of excitation amplitude on the response of the test article.

A triaxial accelerometer measures data in the three mutually perpendicular directions at the top of the solid mass. A uniaxial accelerometer attached to the baseplate is used to control the input to the structure. The data measured at the triaxial accelerometer at the top of the solid mass and the control accelerometer are used to calculate transfer functions between the responses of the three different axes at the top of the solid mass and the input accelerations. The maximum amplitude of the transfer function gives Q, the amplification factor of the input at the natural frequency. The amplification factor, Q, can then be used to calculate the energy dissipation of Ministack using Eq. 31.1 derived in [15].

$$\frac{\pi * Q * A_b^2}{f_n^2} \tag{31.1}$$

Where f_n is the natural frequency of the first axial mode in Hz, A_b is the amplitude of the excitation in g's and Q is the amplification factor of the response.

A configuration is comprised of one set of the two lengths of foam cups and one of the three solid masses. A test series was run for all possible combinations. Between series of tests on each configuration, the setup was disassembled and then reassembled. This reassembly allows for determination of the assembly to assembly variation of the response of the test article. The test sequences are enumerated in Table 31.1. In all assemblies in Table 31.1, the sequence of tests was always repeated to determine if vibrating the specimen changed the dynamic characteristics. The final test assembly 3 was run to see if the order in which the amplitudes were applied affected the dynamics.

Table 31.1 Test sequence

Assembly number	Sweep series amplitudes
1	1 g, 2 g, 5 g, 10 g, 1 g, 2 g, 5 g, 10 g
2	1 g, 2 g, 5 g, 10 g, 1 g, 2 g, 5 g, 10 g
3	10 g, 2 g, 5 g, 1 g, 10 g, 5 g, 2 g, 1 g

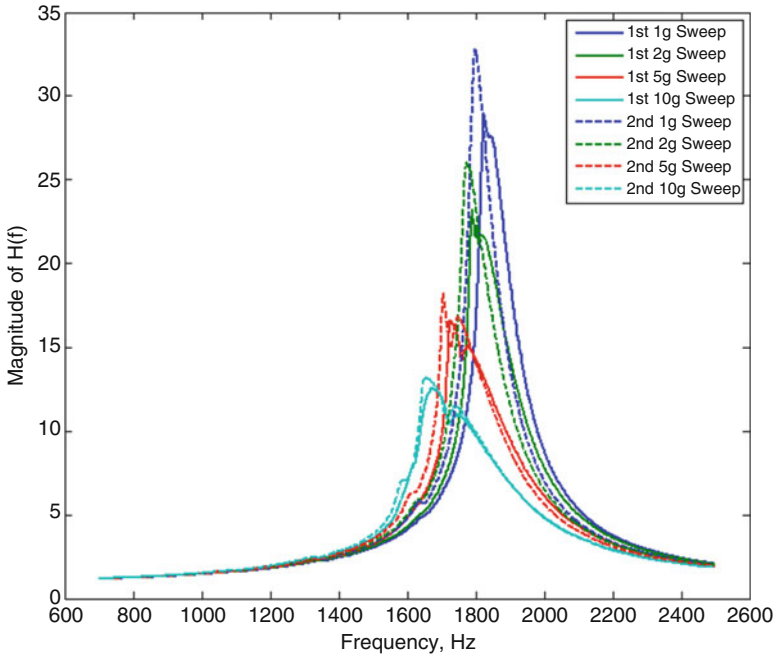

Fig. 31.2 Transfer functions for a specimen preloaded to 3110 N through foam and cylinder, assembly 1

31.3 Experimental Results

31.3.1 Effects of Amplitude of Excitation

This subsection shows the resulting transfer functions for the three test sequences in Table 31.1 on the configuration with the foam cup depth of 5 cm and the solid mass diameter of 7.62 cm (i.e. no gap). In this configuration, the load path goes through both the foam and the solid mass and the solid mass fits snugly into the foam cups. The results for the test sequences shown in Figs. 31.2, 31.3 and 31.4 show that the natural frequency decreases and the amount of energy dissipation increases as the excitation amplitude increases. The frequency shifts suggest that the foam to metal interface loses stiffness at high excitation levels, likely due to micro- or possibly macroslip. The impacts and the friction between the frictional interfaces introduces nonlinear energy dissipation observed at higher excitation levels.

When starting the test series at 1 g and increasing the amplitude to 10 g, the natural frequency from the second run is lower than the first; and the amount of energy dissipation is lower. These phenomena are seen in the data in Figs. 31.2 and 31.3. When starting the test series at 10 g and decreasing the amplitude down to 1 g, there is no appreciable difference in the natural frequency and energy dissipation as seen in Fig. 31.4. One hypothesis for this behavior could be attributed to the higher amplitude sine sweeps causing wear or loss of preload in Ministack. Going from the 1 g to 10 g sweeps and repeating, the settling position of the solid mass after the 10 g run may be different than the initial 1 g run. This could explain why the stiffness and the damping in the transfer functions during the second runs shifted a noticeable amount.

31.3.2 Effects of Snugness of Fit

In this section, the estimated natural frequencies and normalized energy dissipation values are evaluated for different diameters of the solid mass; in other words, how snugly the mass fits into the foam cups. These parameters are plotted

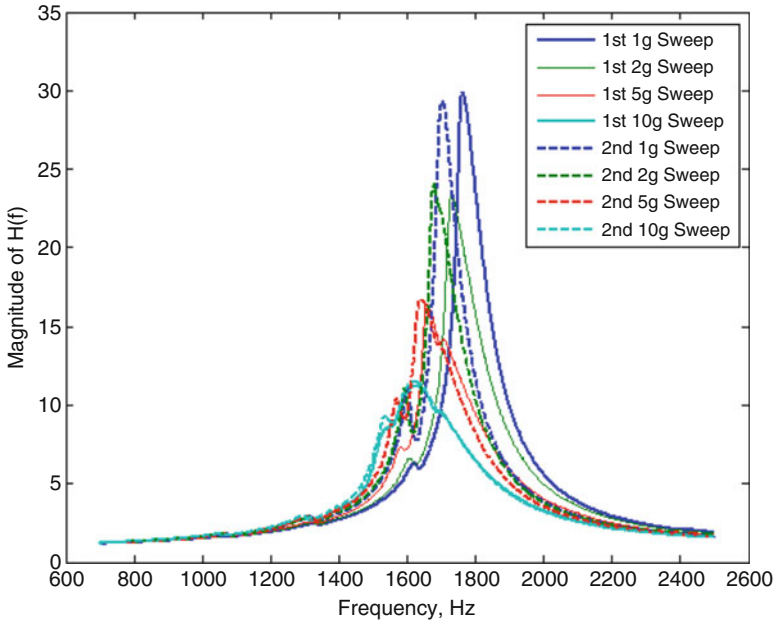

Fig. 31.3 Transfer functions for a specimen preloaded to 3110 N through foam and cylinder, assembly 2

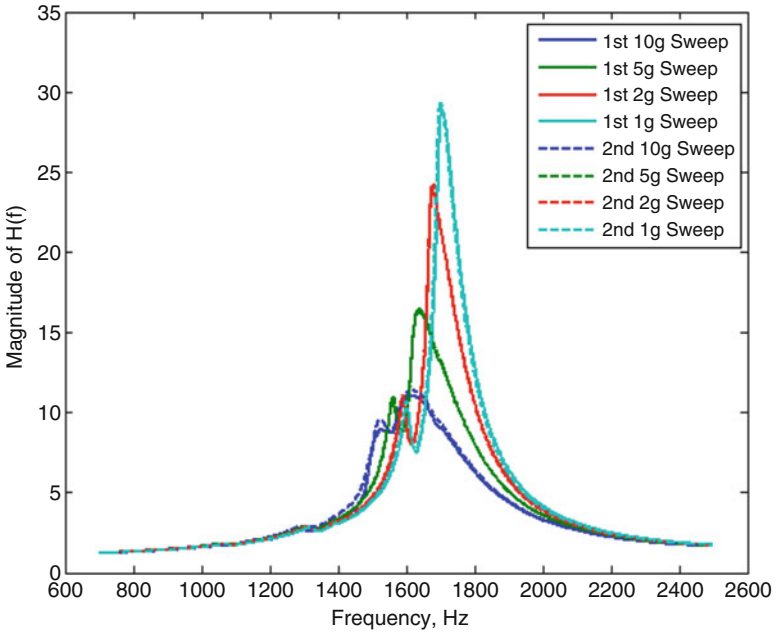

Fig. 31.4 Transfer functions for a specimen preloaded to 3110 N through foam and cylinder, assembly 3

versus the excitation amplitude, because these parameters were shown to be amplitude dependent in the previous subsection. The plot in Fig. 31.5 shows the distribution of the natural frequency for all three gap sizes with the 5 cm depth foam cups, for which the 3110 N preload goes through both the foam and cylinder. The results in Fig. 31.6 show the distribution of the natural frequency with the preload path through the cylinder only (cup depth of 4.68 cm).

Regardless of the load path, the snugness of fit has no statistically significant effect on the variance of the natural frequency, indicating gap size does not affect the repeatability of the assembly process. When the load path goes through both the mass and the foam, the snugness of fit has an impact on the natural frequency. When the gap size is 1.5875 mm, the natural frequency is higher than when there is no gap. The natural frequencies are lower when the gap size is 3.175 mm than either of the other two gap sizes. When the load path goes through the mass only, the snugness of fit has no appreciable effect on the variance of the natural frequency. Additionally, the natural frequency is higher in the case where there is no

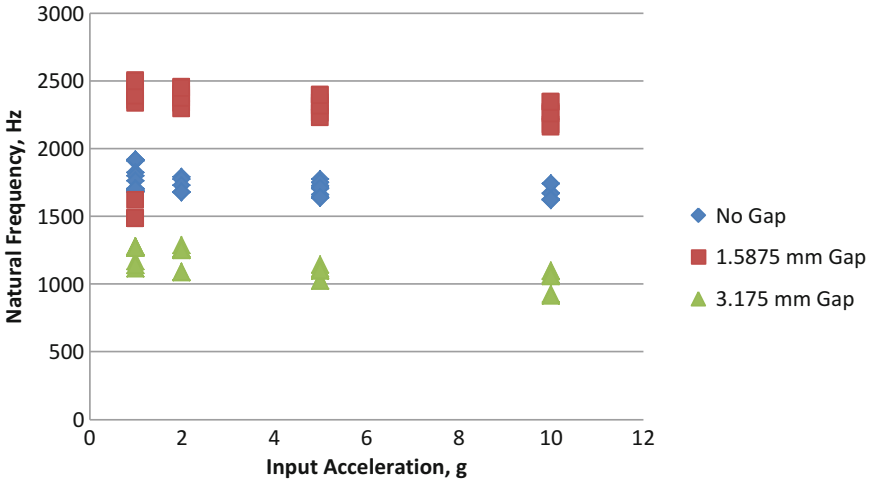

Fig. 31.5 Distribution of natural frequency per gap size with a 3110 N preload through the foam and cylinder

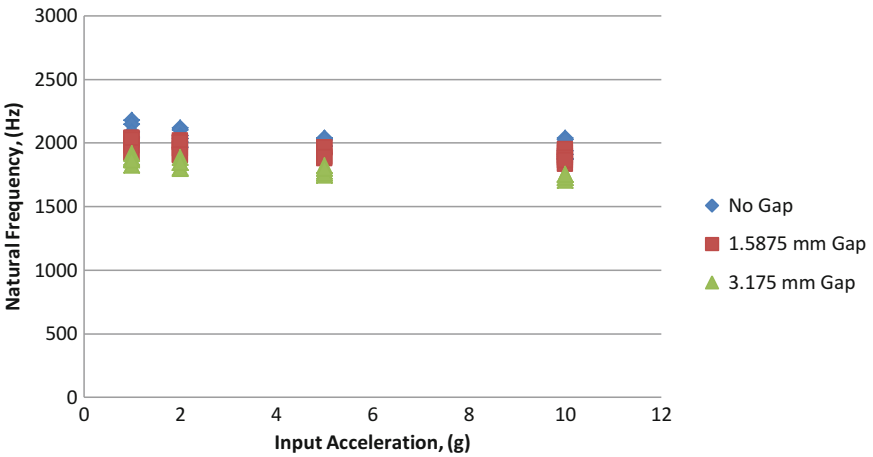

Fig. 31.6 Distribution of natural frequency per gap size with a 3110 N preload through the cylinder only

gap than in the cases where there are gaps. These results suggest that the snugness of fit has a larger effect on the stiffness of the system when the load path goes through the mass and the foam than when the load path goes through the mass only. Additionally, the uncertainty of the natural frequency is larger in the case of the preload going through the mass and the foam, For modeling implications, if the item does not fit snugly in the foam, it is not critical to know how loose it is to determine the natural frequency of the foam/item system when the load path is through the part alone.

The second parameter studied is the energy dissipation. Figure 31.7 shows the distribution of the energy dissipation when the preload for specimens has a load path through the cylinder and foam (5 cm cup depth). Figure 31.8 shows the data for a load path through the cylinder only. A power line is fit to the data to determine the slope of the relationship between energy loss per cycle and the input acceleration. The amount of energy dissipation when the specimens that are preloaded through the foam and cylinder is greater for the specimens that include a radial gap than the specimens that contained no radial gap. The amount of energy dissipation when the specimens are preloaded through the mass only is larger for the case of the specimen with the 3.175 mm radial gap.

These results show that the snugness of fit has an effect on the energy dissipation. The amount of energy dissipated when the specimens are preloaded through the foam and cylinder is greatest when there is a radial gap. One hypothesis for this could be that when there is no gap between the foam and solid mass, the large amount of sliding friction prevents the mass from moving within the container. However, when this large frictional interface is removed with a radial gap, the mass has less resistance to motion and is more likely to impact with the top and bottom surfaces of the foam; these impacts likely dissipate energy differently than sliding friction alone. There will still be some friction along the length of the mass, due to contact along the sides. Additionally, the mass is able to slide laterally with the cross-axis motion of the shaker, introducing a different frictional interface. Finally, the mass and foam are no longer confined as they are when the mass snugly fits in

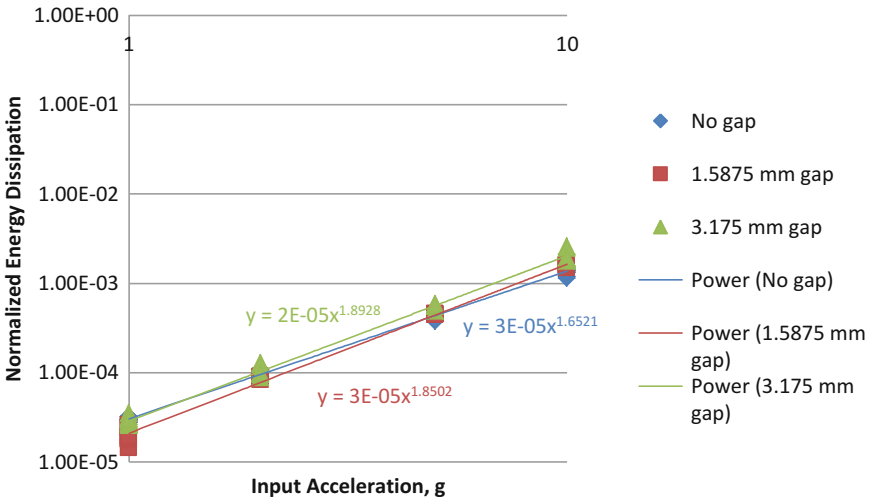

Fig. 31.7 Distribution of normalized energy dissipation per gap size with a 3110 N preload through the foam and cylinder

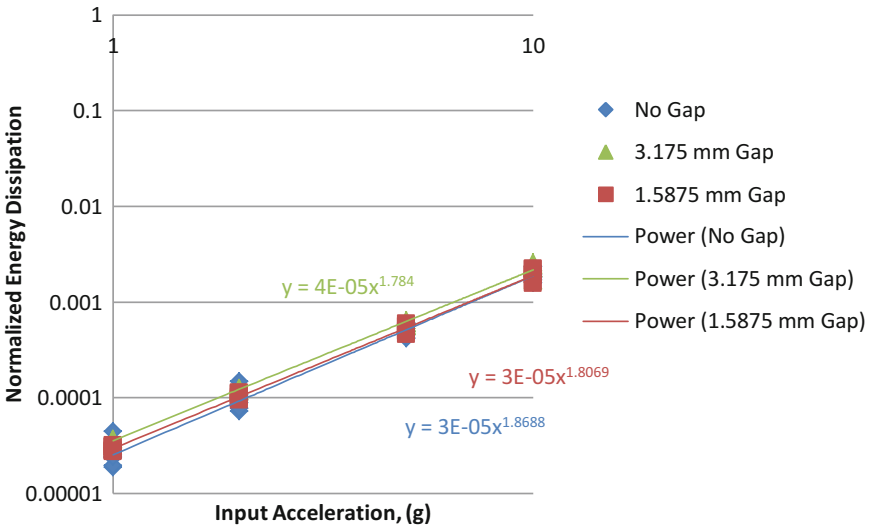

Fig. 31.8 Distribution of normalized energy dissipation per gap size with a 3110 N preload through the cylinder only

the foam, allowing for additional motion and deformation of the foam and mass due to the lack of confinement. In summary, there are additional mechanisms of energy dissipation that occur when there is a radial gap, so it is not surprising that there is more energy dissipation in those cases. The results for the preload going through the cylinder only indicate that again the largest amount of dissipation occurs when the specimen has a 3.175 mm radial gap. For modeling implications, these results suggest that it is important to understand the amount of friction that occurs between the contacting surfaces but also the coefficient of restitution for impacts.

As done in previous studies [3–12], the normalized energy dissipation is plotted vs. the input acceleration on a log–log plot. The data show the anticipated straight line, indicating a power law relationship between energy loss per cycle and the input acceleration. In the fitted results, the slope ranges from 1.65 to 1.89, where 2 is the theoretical value for a linear system with contact friction [3].

31.4 Numerical Results

31.4.1 Computational Model

A high fidelity finite element model was created in Sierra/SD to predict some of the nonlinear behavior observed during the experiments. A mesh of Ministack is shown in Fig. 31.9a; the geometry has the same dimensions as the experimental hardware. There are a total of 198,856 8-noded hexahedral elements, and 15,888 beam elements resulting in a total of 214,744 elements. The hexahedral elements model all the component materials (i.e. ring nut, cover plate, outer can, foam cups, solid mass) with linear elastic properties, as given in Table 31.2. The model assumes that the foam cups behave as a linear elastic material, and a modal damping model accounts for the material damping. We assume that a majority of the nonlinear energy dissipation occurs at the interface between the inner solid mass and the inner surface of the foam cups as shown in Fig. 31.9b. All the beam elements in the model are abnormally stiff beams that rigidly tie the interfacing surfaces of either the solid mass or foam cups to a single node. From this model, two Craig-Bampton reduced order models (ROMs) [13] are created; one of the solid mass and one of the rest of the foam/can assembly. The solid mass has three boundary nodes (top and bottom gap interface, one Iwan interface), resulting in a total of 18 constraint modes. The high stiffness of the solid mass required only a single fixed-interface mode. The foam/can assembly has 4 boundary nodes with the additional one being an excitation node at the base plate of the can. Keeping 20 fixed-interface modes gives this subcomponent ROM a total of 39 degrees-of-freedom. The modal damping values were set to 0.5 % for the solid mass and 2.0 % for the can/foam assembly.

The three boundary nodes of the ROMs are connected to the respective nodes using a single joint element having six different constitutive models for each of the nodal DOF (3 transverse and 3 rotational). The top and bottom interfaces between the solid mass and the corresponding inner surfaces of the foam cups are modeled with a gap element (i.e. piecewise linear spring) in only the y-direction. The parameters for the unloaded and loaded stiffness K_u and K_l, respectively, and the initial gap opening U_0 are given in Table 31.3. No other constitutive models are applied to the top and bottom interfaces. The outer radial surface of the solid mass is tied to a joint element with a four-parameter Iwan model [14] in the y-direction, and stiff elastic springs in all the other directions. The stiffness parameters K_T and K_l were adjusted to best match the 1 g test data in Fig. 31.4 as this was nearest to a linear response. The rest of the parameters were manually adjusted to in order to best align with the repeatable transfer functions at the various excitation levels in Fig. 31.4.

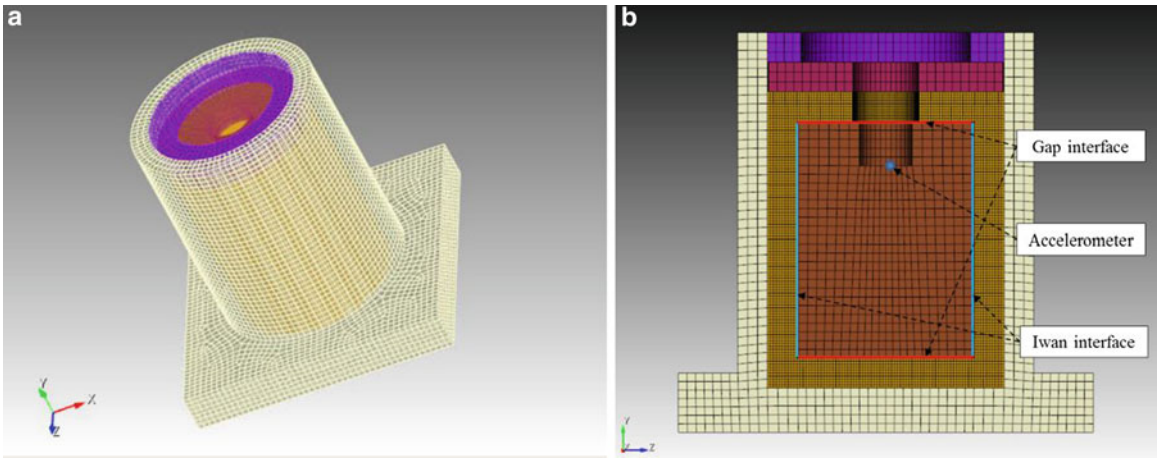

Fig. 31.9 (**a**) Finite element model of Ministack, (**b**) solid mass to foam interface

Table 31.2 Linear elastic material properties

Material	Component(s)	Young's modulus	Density	Poisson's ratio
Aluminum 6061-T6	Slug, outer can	68.9 GPa	2640 kg/m^3	0.33
Structural steel	Ring nut, cover plate	207 GPa	7705 kg/m^3	0.33
PMDI	Foam cups	162 MPa	289 kg/m^3	0.30

Table 31.3 Parameters in nonlinear joint elements

	Parameters			
Element	K_u	K_l	U_0	–
Top & bottom gap	0.0 lbf/in	1.0 E + 06 lbf/in	0.0 in.	–
	Parameters			
	K_T	F_s	B	χ
Iwan	2.0 E + 06 lbf/in	100.0 lbf	0.0	−0.5

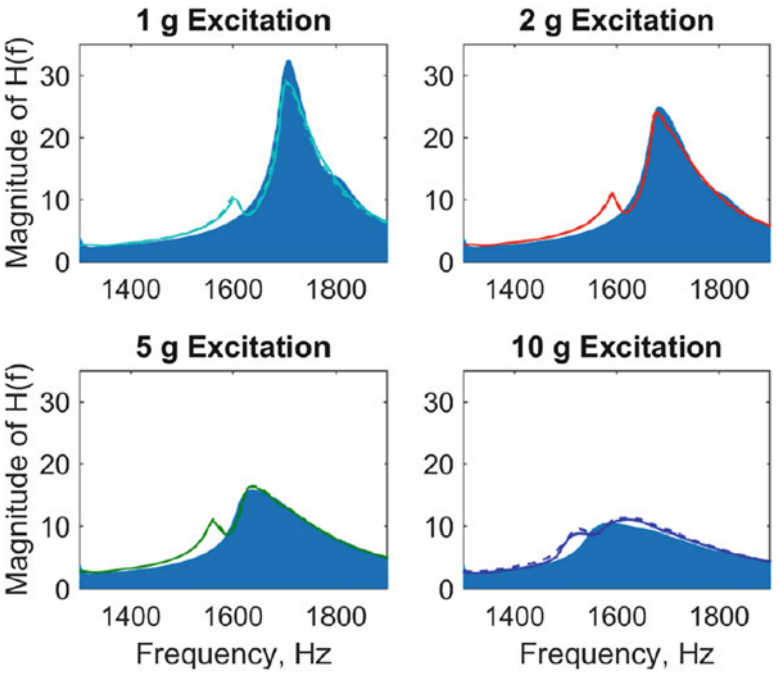

Fig. 31.10 Comparison of experimental transfer functions and simulated sine sweeps from 10 g to 1 g

31.4.2 Comparison Between Model and Experiments

The assembled ROMs with nonlinear connections were subject to an upward sine sweep excitation from 1300 to 1900 Hz at a sweep rate of 750 Hz/s. Each sweep applied a base acceleration in the y-direction at various amplitudes (1 g, 2 g, 5 g, and 10 g) in order to excite the first axial mode of Ministack. The objective of the simulation was to identify the appropriate constitutive parameters in Table 31.3 that correlate with the measured transfer functions shown in Fig. 31.4. This experimental data was chosen since it was repeatable and did not depend on prior test runs. The simulated sweeps are overlaid onto the experimental data in Fig. 31.10. The solid mass exercises the Iwan interface since the excitation sweeps through the frequency of the first axial mode. The model captures a loss of stiffness of 1708 Hz at a 1 g load down to 1585 Hz at 10 g's. The peak of the transfer function also decreases as the load amplitude increases, suggesting that the amount of energy dissipation in the Ministack is reasonably captured with the Iwan element. In future efforts, the model will be updated to capture the bi-modal hump seen in the test data as this phenomenon is likely due to the loss of contact between the solid mass and the foam.

31.5 Conclusions

A series of upward sine sweeps are run on Ministack, which is a simple system representing a metal component packaged in foam. The measured results give insight into the influence of input amplitude, snugness of fit, load path and sequence of testing on the energy dissipation and natural frequency in the system. As the amplitude of excitation increases, the natural frequency decreases and the amount of energy dissipated each cycle increases. The foam to metal interface seems to be

responsible for this behavior due to friction, impact, loss of preload, and material damping. The nonlinear nature of these physics presents itself in the measured transfer functions and estimated parameters.

The first set of results show the effect of the order of the amplitudes of the sine sweeps. When the sine sweeps start at a low amplitude and increase, the natural frequency from the second run shifts to a lower frequency in comparison to the first run. Similarly, the amount of energy dissipation is lower on the second run. When starting the test series at a high amplitude and decreasing the amplitude there was no appreciable difference in the parameters. Starting the run with a 10 g load case may cause the mass to initially settle and lose some of its preload, which could explain why the order of sweep amplitude influence the behavior.

Three different size solid masses were tested along with sets of foam cups with two different depths, which changes the load path of the preload. Regardless of the load path, the snugness of fit has no statistically significant effect on the variance of the natural frequency, indicating gap size does not affect the repeatability of the assembly process. When the load path goes through both the mass and the foam, the snugness of fit has an impact on the natural frequency. The smaller gap case has higher natural frequencies than the no gap case and the larger gap case has lower natural frequencies than the no gap case. When the load path goes through the mass alone, the natural frequency is higher in the case where there is no gap than in the cases where there are gaps. These results suggest that the snugness of fit has a larger effect on the stiffness of the system when the load path goes through the mass and the foam than when the load path goes through the mass only. Additionally, the uncertainty of the natural frequency is larger in the case of the preload going through the mass and the foam, likely due to the variation in the foam.

The results of this study show that the snugness of fit has an effect on the energy dissipation. Regardless of load path, the amount of energy dissipated is greatest when there is a radial gap. It is likely that the increased energy dissipation in the presence of a radial gap is due to mechanisms of energy dissipation that occur when there is a radial gap in addition to the contact friction that is present when there is no radial gap. For modeling implications, these results suggest that it is important to understand the amount of friction that occurs between the contacting surfaces but also the coefficient of restitution for impacts.

A first attempt at modeling Ministack was done using a Craig-Bampton model connected with various nonlinear elements. The simulated sine sweeps with an Iwan element and two gap elements matched the test data quite well. In future work, other interfaces models will be explored along with a more systematic way of identifying the model parameters from test data.

References

1. U.S. Department of Defense Standard Practice for Military Packaging, MIL-STD-2073-1E w/Change 1, January 2011
2. U.S. Department of Defense Environmental Engineering Considerations and Laboratory Tests, MIL-STD-810G, Oct. 2008
3. Goodman, L.E.: A review of progress in analysis of interfacial slip damping. In: Jerome E Ruzincka (ed.) Structural Dumping, papers presented at a colloquium on structural damping held at the ASME annual meeting in Atlantic City, pp 35–48. NJ (1959)
4. Goodman, L.E., Brown, C.B.: Energy dissipation in contact friction: constant normal and cyclic tangential loading. J. Appl. Mech. **29**, 17–22 (1962)
5. Ungar, E.E.: The status of engineering knowledge concerning the damping of built-up structures. J. Sound Vib. **26**, 141–154 (1977)
6. Metherell, A.F., Diller, S.V.: Instantaneous energy dissipation rate in a lap joint - uniform clamping pressure. J. Appl. Mech. **35**, 333–340 (1968)
7. Groper, M.: Microslip and macroslip in bolted joints. Exp. Mech. **25**, 171–174 (1985)
8. Menq, C.H., Bielak, J., Griffin, J.H.: The influence of microslip on vibratory response, Part 1, a new microslip model. J. Sound Vib. **107**, 279–293 (1986)
9. Gaul, L., Lenz, J.: Nonlinear dynamics of structures assembled by bolted joints. Acta Mech. **125**, 169–181 (1997)
10. Sanliturk, K.Y., Stanbridge, A.B., Ewins, D.J.: Friction dampers: measurement, modelling and application to blade vibration control. ASME Design Engineering Technical Conferences vol. 3, Part B, 1995
11. Rogers, P.F., Boothroyd, G.: Damping at metallic interfaces subjected to oscillating tangential loads. J. Eng. Ind. **97**, 1087–1093 (1975)
12. Padmanabhan, K.K., Murty, A.S.R.: Damping in structural joints subjected to tangential loads. Proc. Inst. Mech. Eng. **205**, 121–129 (1991)
13. Craig, R.R.J., Kurdila, A.J.: Fundamentals of Structural Dynamics, 2nd edn, pp. 531–570. Wiley, New York (2006)
14. Segalman, D.J.: A four-parameter Iwan model for lap-type joints. ASME. J. Appl. Mech **72**(5), 752–760 (2005). doi:10.1115/1.1989354
15. Chopra, A.K.: Dynamics of Structures, 2nd edn, pp. 65–118. Prentice Hall, New Jersey (2001)